

Commuter welfare-based probabilistic seismic risk assessment of regional road networks

Rodrigo Silva-Lopez, Gitanjali Bhattacharjee, Alan Poulos, Jack W. Baker

October 3, 2022

Abstract

This study integrates welfare, a measure of the impact of road network disruption on individual commuters’ well-being, with a probabilistic seismic risk assessment framework in a computationally tractable way. Welfare is a network performance measure that reflects the differential impacts of changes in commute time on various groups. For a case study of the San Francisco Bay Area, welfare loss is computed by augmenting an origin-destination matrix with publicly available information about commuters’ income levels, residences, and workplaces. While commuters from all income groups have similar risk of drivers’ delay due to road network disruption, commuters with low incomes have a substantially higher risk of welfare loss than those with high incomes. A comparison of bridge retrofit policies shows that disaggregation of welfare loss by income group is necessary to examine whether such policies reduce risk equitably. While a retrofit policy determined using drivers’ delay reduces the expected drivers’ delay, it increases the disparity in the per-capita welfare loss of commuters with low and high incomes relative to the network’s baseline state. In contrast, a retrofit policy that prioritizes low-income commuters reduces the difference in welfare loss of commuters with low and high incomes compared to the baseline network state.

1 Introduction

Methods for seismic risk assessment and reliability analysis of road networks are diverse in terms of the measures of road network disruption they use as well as their geographical scale, time frame considered (e.g., emergency response or long-term recovery), and the needs they aim to address (e.g., emergency planning, network expansion, risk mitigation) (e.g., Argyroudis et al., 2015; Faturechi & Miller-Hooks, 2015; Werner et al., 2000). Approaches to quantifying the impacts of road network disruption fall into four broad categories of increasing computational complexity: (1) topological approaches characterize the road network using graph theoretic metrics like connectivity, which indicates how well origins and destinations in the network are connected; (2) functional approaches characterize the level of service provided to users of the road network using measures like travel time, travel distance, mode-destination accessibility, and flow; (3) economic approaches estimate the economic losses incurred by post-earthquake road network damage; (4) and well-being-based approaches account for how individuals’ quality of life changes as a result of changes to the road network (Chang et al., 2012; Chang, 2016; Faturechi & Miller-Hooks, 2015; Miller, 2014; Murphy & Gardoni, 2006; Werner et al., 2000).

Seismic risk assessments can use measures of road network disruption directly – for example, travel time is the most commonly used decision variable in the literature on transport infrastructure system performance in disasters (Faturechi & Miller-Hooks, 2015). Measures of disruption can also serve as inputs to a cost model (Argyroudis et al., 2015; Kilanitis & Sextos, 2019b; Werner et al., 2000). Cost models typically sum the cost of restoring the functionality of damaged components (i.e., direct costs) and the costs associated with ongoing network disruption while damaged components undergo repair (i.e., indirect costs) (Dong et al., 2014; Hackl et al., 2018; Kilanitis & Sextos, 2019b; Kiremidjian et al., 2007). Classical sources of indirect costs include travel time delay (the increase in time required to make all trips demanded on the damaged road network compared to normal conditions) and unmet demand (e.g., Decò & Frangopol, 2013; Hackl

et al., 2018). Proposed additions to the category of indirect costs typically focus on societal impacts of road network disruption and the lost economic value of activities (e.g., working or shopping) not performed when trips are not made (Zhou et al., 2010), accidents that result in casualties (Decò & Frangopol, 2013), road network operations (Decò & Frangopol, 2013), carbon dioxide emissions, fatalities following an earthquake (Dong et al., 2014), and energy waste due to repair of damaged components (Dong et al., 2014).

While travel time delay and the cost of road network performance can be useful measures of disruption and relatively practical to implement in terms of computational expense, they may not improve our understanding of how network disruptions impact individuals or different groups of network users. If used as a decision variable, travel time delay implicitly assumes that all travelers have an equal value of time (VoT). VoT quantifies the willingness of a traveler to pay to reduce the time they spend in transit by one unit and is also referred to as the subjective (or behavioral) value of travel time (SVTT), and the subjective (or behavioral) value of travel time savings (e.g., Jara-Díaz & Guevara, 2003; Small, 2012). A traveler may be willing to pay to reduce the time they spend in transit because transit itself has low utility (i.e., they derive little satisfaction or pleasure from transiting) or because they could spend the time saved in more pleasurable or more useful ways (Mackie et al., 2001). VoT can depend on qualities of the trip, such as its purpose (for work or for recreation), mode (e.g., car or bicycle), duration, or the time at which it is made (Mackie et al., 2001; Small & Verhoef, 2007). VoT can also vary depending on the characteristics of travelers themselves, including their individual preferences, demographic characteristics (e.g., age, sex, level of education, employment), and hourly income (Belenky, 2011; Small & Verhoef, 2007). Models of indirect cost in which travel time delay is multiplied by a single VoT to arrive at a monetary loss (e.g., Hackl et al., 2018; Kilanitis & Sextos, 2019a, 2019b; Werner et al., 2000) do not account for variations in VoT associated with travelers’ characteristics. Nor can such models account for how an individual’s marginal utility of income decreases as their income increases – that is, the greater an individual’s income, the less utility they experience as a result of each additional unit of income (e.g., Layard et al., 2008). Variability in the marginal utility of income further complicates efforts to assess in aggregate the value of time spent in transit to commuters.

If the characteristics of travelers that affect their VoT are not accounted for when traffic on the road network is simulated, subsequent disaggregation of travel time delay (or other summary measure of network performance) by those characteristics is not possible. Disaggregation of network performance measures is necessary to conduct equity analysis, the goal of which is to understand how fairly and/or justly the costs and benefits of a particular policy are distributed among members of society, including both users and non-users of the road network (Bills & Walker, 2017; Litman, 2002). Equity analysis is particularly important in light of historically inequitable transport planning processes and outcomes that have resulted in less-advantaged members of society having experienced disproportionately high shares of the costs and disproportionately low shares of the benefits of transport projects (e.g., Bills & Walker, 2017). Furthermore, disasters are widely acknowledged to exacerbate existing societal inequities (e.g., Lindell & Prater, 2003). Assessing and limiting inequities in transport systems in particular has been the subject of state and federal legislation in the US (Bills & Walker, 2017).

How risk assessment methods for road networks account for impacts on different groups of people is therefore of growing concern to researchers. In transport systems, equity has two primary dimensions: horizontal equity considers how impacts are distributed among groups deemed equal in ability and need, while vertical equity considers how impacts are distributed among groups that differ in ability and need, e.g., people of different income levels (Bills & Walker, 2017). For example, Miller and Baker (2016) conduct a vertical equity analysis by examining how an individual’s income class (low, medium, high, or very high) and their household’s ratio of cars to workers affect their expected post-earthquake mode-destination accessibility decrease in the San Francisco Bay Area. Boakye et al. (2022) propose a method for assessing spatial inequalities in the impacts of a hazard on individuals’ abilities to engage in activities that improve their well-being, e.g., “Earning Income”, “Being Educated”, and “Being Mobile”, following the Capabilities-Based Approach (Murphy & Gardoni, 2006).

In this work, we aim to better characterize the impacts of post-earthquake road network disruption on individual network users within a probabilistic seismic risk assessment framework. We use welfare loss (as

formulated by Galvez & Jara-Diaz, 1998) to characterize road network performance. Welfare loss (in units of utils) describes the value to society of individual travelers’ increased travel times and is a function of increased travel times as well as travelers’ personal SVTT, their marginal utilities of income, and the value placed by society on the utility of individual travellers (Mackie et al., 2001). As a summary statistic of network performance, welfare takes into account that the same change in commute time can impact commuters with different characteristics in different ways. Because welfare loss takes into account the satisfaction (or utility) of the individual traveler, it falls into category (4) of measures of road network disruption outlined above. Setting up the seismic risk assessment of a road network such that welfare losses can be computed also enables the disaggregation of summary statistics such that the impacts of disruptions on different groups can be articulated – a prerequisite for devising more equitable network management policies. Importantly, welfare loss is computationally tractable within a probabilistic framework and can be computed using publicly available data, as we show in this study.

The remainder of this work is organized as follows. In Section 2, we detail the probabilistic seismic risk assessment procedure as well as the computation of welfare loss. In Section 3, we carry out a probabilistic seismic risk assessment of the San Francisco Bay Area using welfare loss as a measure of the road network disruption caused by damage to highway bridges. We compare the insights possible using welfare loss to those possible using travel time delay and demonstrate how these measures can inform risk mitigation policies. Section 4 provides discussion and conclusions.

2 Methods

By integrating welfare loss, previously described by Galvez and Jara-Diaz (1998) and Mackie et al. (2001), with an established probabilistic seismic risk assessment framework, we investigate how earthquake-induced highway bridge damage impacts commuters in different income groups and compare the results of a welfare loss-based risk assessment with those of a delay-based risk assessment. Figure 1 summarizes the process by which welfare loss can be computed, as well as the input data and models required, for a single earthquake rupture scenario. In the following subsections, we detail each step of Figure 1 in the context of a probabilistic seismic risk assessment procedure.

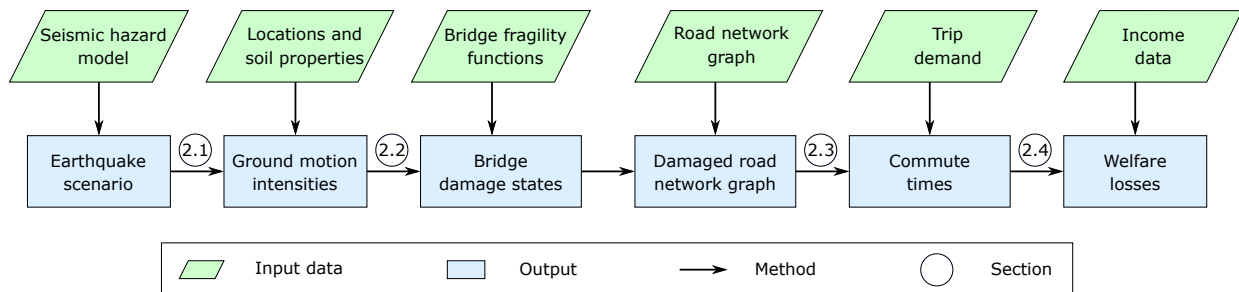


Figure 1: Diagram summarizing the evaluation of the impact of an earthquake scenario on the users of a road network.

2.1 Ground-motion intensity maps

We first use a seismic source model to generate n_S earthquake scenarios that are consistent with the seismic hazard of the region in which the road network is located. A seismic source model provides the rates, locations, faulting types, and magnitudes of earthquakes that can occur in the area. For each earthquake scenario, a ground-motion model (GMM) is used to model the ground-motion intensity IM at each bridge b . A GMM predicts the mean of the log ground-motion intensity ($\ln Y$) as well as the ground-motion intensity within- (σ) and between-event (τ) residual standard deviations. GMMs are typically the function of many

inputs, including the moment magnitude of the earthquake scenario, a metric of distance from a given location to the fault plane, and the average shear wave velocity down to 30 meters. For each of the n_S earthquake scenarios, m ground-motion intensity maps can be sampled by sampling m realisations of the spatially-correlated ground-motion intensity residual terms (see, e.g., Han and Davidson, 2012 for a survey of sampling methods). The set of $N = n_S \times m$ ground-motion intensity maps is indexed using j (i.e., $j = 1, \dots, N$). Given the residuals, the total log ground-motion intensity at a bridge b in a particular map j can be computed per Equation (1),

$$\ln Y_{bj} = \overline{\ln Y(M_j, R_{bj}, V_{s30,b}, \dots)} + \sigma_{bj}\varepsilon_{bj} + \tau_j\eta_j \quad (1)$$

where σ_{bj} is the within-event residual standard deviation, ε_{bj} is the normalised within-event residual in $\ln Y$, τ_j is the between-event residual standard deviation, η_j is the normalised between-event residual in $\ln Y$, M_j is the moment magnitude of the earthquake scenario associated to ground-motion intensity map j , R_{bj} is the distance between location b and the fault plane of ground-motion intensity map j , and $V_{s30,b}$ is the average shear wave velocity down to 30 meters at the b^{th} location. Both ε_{bj} and η_j are standard normal random variables. ε_{bj} represents location-to-location variability, and its vector can be modelled using a spatially-correlated multivariate normal distribution. η_j represents between-event variability, and its vector can be modelled using a standard univariate normal distribution. The result of this procedure is a set of N ground-motion intensity maps. The annual rate of occurrence for the j^{th} ground-motion intensity map, ω_j , is the original rate of occurrence of the associated earthquake scenario divided by m , since m ground-motion intensity maps are simulated per earthquake scenario.

2.2 Damage maps

For each ground-motion intensity map n , we sample a damage map, i.e., a vector of n_B binary variables, each of which indicate the functionality of a particular bridge. The probability that a bridge experiences a damage state that reduces its normal functionality, given a particular ground-motion intensity, can be quantified using a fragility function, as given in Equation (2),

$$P(DS_{bj} \geq ds | Y_{bj} = y) = \Phi \left(\frac{\ln \frac{y}{f_b}}{\beta_b} \right) \quad (2)$$

where Y_{bj} denotes the ground-motion intensity at bridge b in ground-motion intensity map j , Φ is the standard normal cumulative distribution function, and $\ln f_b$ and β_b are the mean and standard deviation, respectively, of the $\ln Y_b$ value required to cause the damage state of interest ds to occur or be exceeded for the b^{th} bridge. Bridge damage results in the partial or total closure of the roads carried by the damaged bridge.

2.3 Model of road network performance

Traffic models typically comprise four sequential sub-models for trip generation, trip distribution, modal split, and traffic assignment (Patriksson, 2015). In the case study of Section 3, we use a simplified traffic model in which the trip generation, distribution, and modal split sub-models are replaced by publicly available empirical data on commuters’ residences and places of work at the census block level. In this section, we briefly describe the simplified traffic assignment procedure used in the case study. This simplified model is not a prerequisite for integrating welfare loss with a probabilistic seismic risk assessment procedure: other, more sophisticated traffic models (such as activity-based models) may be appropriate, depending on the analysis objectives and resources.

2.3.1 Traffic assignment model

A traffic assignment model takes a graph of the road network, G , and the demand between a set of origins and destinations as inputs and returns one or more measures of road network performance, such as aggregate travel time, aggregate vehicle-miles travelled, and the number of trips made. The graph of the road network

is directed and comprises a set of vertices, V , and a set of edges, E , connecting them: $G = (V, E)$. Each edge $e \in E$ has associated properties – e.g., length, capacity in vehicles per unit of time, free-flow traversal time, and flow (i.e., number of vehicles assigned to it) – that determine the rate at which traffic can pass over it. The flow on an edge can be determined using a traffic assignment algorithm, which allocates trips to edges according to some rule. A common rule is to assign trips to the shortest-time path between an origin and destination. Assigning trips to the edges that comprise a path will modify the properties of those edges, e.g., increasing their traversal times. The minimum definition of the demand on the road network is an origin-destination matrix, typically a two-dimensional array in which each element is the number of trips demanded between a particular origin and destination in a certain time period.

2.3.2 Road network performance

Once all trips have been assigned to the road network, we can compute the aggregate travel time, T , using Equation (3),

$$T = \sum_{e \in E} q_e t_e \quad (3)$$

where e is an edge in the network, E is the set including all edges, q_e is the flow over edge e , and t_e is its traversal time. The change in aggregate travel time on a version of the road network that includes damaged bridges compared to the undamaged road network, ΔT , can be computed by subtracting T when the network is undamaged from T as computed given a damage map. ΔT is also called drivers’ delay.

The travel time between a particular origin and destination along the shortest-time path P_{OD} in the undamaged road network is given by Equation (4),

$$t_{OD} = \sum_{e \in P_{OD}} t_e \quad (4)$$

where P_{OD} is the shortest-time path linking the origin O and destination D . The change in travel time between an origin and a destination, Δt_{OD} , is given by Equation (5),

$$\Delta t_{OD} = \sum_{e \in P'_{OD}} t'_e - \sum_{e \in P_{OD}} t_e \quad (5)$$

where P'_{OD} denotes the shortest-time path in the new (damaged) graph of the road network. Equation (5) is needed to compute welfare loss.

2.4 Welfare model

Equation (6) gives the welfare model of Mackie et al. (2001),

$$\Delta W_i = \Omega_i \lambda_{u,i} SVTT_i \Delta T_i \quad (6)$$

where ΔW_i denotes the change in welfare among commuters in income group i , Ω_i is a weight assigned to group i , $\lambda_{u,i}$ is the marginal utility of income for members of group i , $SVTT_i$ is the subjective value of travel time for members of group i , and ΔT_i is the change in the aggregate travel time of members of group i .

In this model, the change in a network user’s travel time is weighted by factors that account for how valuable the time saved or additional time spent commuting is to the particular user, as determined using information about their individual earnings. This welfare model can be used with traffic models of varying sophistication, from the simplified traffic assignment model used in the example of Section 3 to more sophisticated activity-based travel demand models that planners may wish to use. To assess welfare loss, we use an augmented origin-destination matrix in which each trip is associated with information about the individual earnings of the person making the trip, namely, to which income group q they belong.

With the exception of ΔT_i , which is an output of the traffic assignment algorithm, all of the parameters in Equation (6) must be defined by the analyst. The definition of income groups depends on the available

data. In the example of Section 3, commuters belong to one of three income groups as determined using a publicly available data set. Ω reflects how a society values equity. Per Mackie et al. (2001), $\Omega_i = 1$ for all i is typically used to evaluate projects in the United States of America. The marginal utility of income, λ_u , is a key parameter in developing policies through cost-benefit analysis (Layard et al., 2008). λ_u allows an analyst to weight any change in a person’s income that result from a policy by the resulting change in their utility (e.g., Layard et al., 2008). To derive λ_u , we first need a model for the utility u of income y . Layard et al. (2008) give one such model in Equation (7),

$$u = \begin{cases} \log(y) & \text{if } \rho = 1 \\ \frac{y^{1-\rho}-1}{1-\rho} & \text{if } \rho \neq 1 \end{cases} \quad (7)$$

where ρ is the elasticity of λ_u . We can then derive λ_u as shown in Equation (8).

$$\lambda_u = \frac{\partial u}{\partial y} = \frac{1}{y^\rho} \quad (8)$$

Equation (9) gives a common estimate of SVTT, where y is the commuter’s wage rate in monetary units per hour (Small, 2012).

$$SVTT = \frac{1}{2}y \quad (9)$$

Note that SVTT is dependent on a person’s earnings, which comprise only the wages a person earns by working and are a subset of an individual’s income, which may also include interest, dividends, and benefits (e.g., Hallegatte et al., 2016). However, in this work, we treat individual earnings and income as interchangeable given the data available for the example of Section 3. We therefore use the term “income” for simplicity throughout this paper.

In general, changes in welfare can be computed for the spatial unit of interest using Equation (10), which yields the change in welfare for all trips from an origin, and Equation (11), which yields the change in welfare for all trips to a destination. In both Equations (10) and (11), O denotes an origin, D denotes a destination, $d_{OD,i}$ denotes the demand from O to D among members of income group i , and Δt_{OD} is given by Equation (5).

$$\Delta W_{O\bullet} = \sum_D \sum_i \Omega_i \lambda_{u,i} SVTT_i d_{OD,i} \Delta t_{OD} \quad (10)$$

$$\Delta W_{\bullet D} = \sum_O \sum_i \Omega_i \lambda_{u,i} SVTT_i d_{OD,i} \Delta t_{OD} \quad (11)$$

In Section 3, we compute welfare losses for each census block in the region of interest using Equations (10) and (11). The total change in welfare, ΔW , for an area of interest can be computed by summing the welfare change experienced by each income group: $\Delta W = \sum_i \Delta W_i$.

Finally, the results of all ground-motion intensity maps are aggregated using Equation (12) to compute the expected annual welfare loss,

$$\mathbb{E}[\Delta W] = \sum_{j=1}^N \omega_j \Delta W_j \quad (12)$$

and using Equation (13) to compute the mean annual rate of exceedance of the welfare loss,

$$\lambda_{\Delta W}(x) = \sum_{j=1}^N \omega_j \mathbb{1}(\Delta W_j \geq x) \quad (13)$$

where N is the number of ground-motion intensity maps considered, ω_j is the annual rate of occurrence of ground-motion intensity map j , ΔW_j is the welfare loss associated with ground-motion intensity map j , and $\mathbb{1}(\Delta W_j \geq x)$ is an indicator function that evaluates to 1 if ΔW_j exceeds x , a welfare loss threshold of interest, and to 0 otherwise.

3 Case study: San Francisco Bay Area

We conduct a probabilistic seismic risk assessment of the nine-county San Francisco Bay Area road network in which disruption is measured using drivers’ delay (ΔT), welfare loss (ΔW), and welfare loss per commuter (Δw). The San Francisco Bay Area is a region of high seismic hazard (Petersen et al., 2020) that contains 1743 highway bridges owned and managed by the California Department of Transportation (Caltrans) and which are modeled as the vulnerable elements of the road network. We first detail the implementation of the methods described in Section 2 to simulate ground motions, damage maps, traffic, and changes in commuter welfare in Section 3.1. In Section 3.2 we present and discuss results for the expected welfare loss ($\mathbb{E}[\Delta W]$) and expected welfare loss per commuter ($\mathbb{E}[\Delta w]$) and compare the resulting insights with those available from an analysis using drivers’ delay (ΔT). Through an example application to the problem of bridge retrofit prioritization, we show how using welfare (rather than time) as a measure of network performance can indicate differing impacts of network disruption on groups of commuters. The particular models used and assumptions made in this example are not necessary to apply the proposed methods.

3.1 Implementation

3.1.1 Ground-motion intensity maps

We use OpenSHA (Field et al., 2003) with the UCERF2 seismic source model (Field et al., 2009), Wald and Allen’s topographic slope model for the shear wave velocity (V_{s30}) value (Wald & Allen, 2007), and the ground motion model developed by Chiou and Youngs (2014) to generate an earthquake rupture forecast comprising 6577 scenarios (i.e., median ground-motion intensity measure fields). For each scenario, we then simulate spatially correlated ground motions at all 1743 bridges using the model proposed by Jayaram and Baker (2009). (With respect to Section 2.1. The ground-motion intensity measure for the maps used to simulate bridge damage is the 5%-damped pseudo absolute spectral acceleration (S_a) at a period of 1 second, the required input to the bridge fragility functions provided by Caltrans (Miller, 2014). To reduce the computational burden of simulating network performance, we select a hazard-consistent subset of $n_S = 1980$ ground-motion intensity maps from the original set of scenarios using an optimization procedure developed by Han and Davidson (2012) and by Miller (2014).

3.1.2 Damage maps

We create one damage map per scenario by sampling bridges’ damage states using their associated fragility functions, of the form given in Equation (2), with parameters from Miller (2014). We model both extensive and complete bridge damage as necessitating complete closure of the carried road and any associated underpasses. Closures are modeled as modifications of edge properties in the graph of the road network as detailed in Section 3.1.3. Minor and moderate damage states are not modeled as affecting traffic, which is consistent with the functional characterization described by Werner et al. (2006) after the emergency response phase. The spatially correlated ground motions will lead to spatial correlations in bridge damage. No further modeling of damage correlations, conditional on S_a , are included.

3.1.3 Road network performance

The San Francisco Bay Area road network is modeled as a directed graph $G = (V, E)$ and shown in Figure 2 (Miller, 2014). Each of the 1743 state-owned highway bridges in the region is associated with one or more edges in the graph. Each edge in E has a traversal time given a traffic volume according to the commonly used Bureau of Public Roads (1964) travel time function,

$$t_a = t_f \left(1 + 0.15 \left(\frac{q_a}{c_f} \right)^4 \right) \quad (14)$$

where t_f is the free-flow travel time, t_a is the capacity-dependent travel time, c_f is the hourly capacity, and q_a is the hourly flow on the edge. To model a complete road closure due to a damaged bridge, the associated edges are modified to have an hourly capacity $c_f = 0$ and free-flow and capacity-dependent travel times

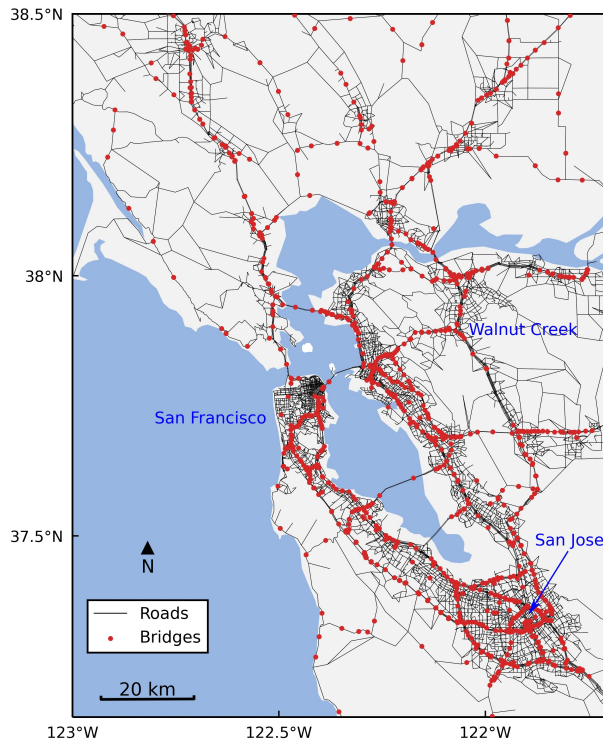


Figure 2: Map of the San Francisco Bay Area road network used in this study.

$t_f, t_a = \infty$, which ensures no trips use those edges.

We obtain the demand on the road network from the Longitudinal Employer-Household Dynamics Origin-Destination Employment Statistics (LODES) data set, Version 7.5 (U.S. Census Bureau, 2010). The LODES data set tabulates the census block in which a commuter lives, the census block in which they work, and their membership in one of three income groups (low, medium, or high) based on their annual individual earnings (U.S. Census Bureau, 2010). We can therefore define an origin-destination matrix for the region of interest in which each trip is associated with the income group of the commuter demanding it. We discuss our characterization of commuters in Section 3.1.4. Since the edge capacities of the links in G are hourly, we scale the daily demand by a factor of 0.21 to get the hourly demand during the 6 am - 10 am window, a peak commuting time (Wang et al., 2012). We assume that commuters’ travel preferences are invariant before and after an earthquake, a common assumption (e.g., Hackl et al., 2018). However, a commuter whose trip exceeds the maximum acceptable one-way commute time, t_{max} , will forgo said trip. In this example, $t_{max} = 4$ hours. This is consistent with the assumption that in a 24 hour period, commuters work 8 hours and rest 8 hours (Belenky, 2011). The welfare loss that results from a trip’s duration exceeding t_{max} on the damaged road network is computed based on a travel time increase equal to the difference of t_{max} and the trip’s duration on the undamaged road network.

We implement an iterative traffic assignment (ITA) algorithm that divides the demand into parts comprising 40%, 30%, 20%, and 10% of the total trips demanded (Beckmann et al., 1956). It assigns the first 40% of the trips to the shortest path, in terms of the sum of the traversed edges’ free-flow travel times t_f , between the origin and destination. The shortest path is found using Dijkstra’s algorithm. The link flows q_a are updated to reflect the assigned trips, and the capacity-dependent travel times t_a are updated according to Equation (14). The ITA algorithm then assigns each remaining portion of the demand in a similar fashion; at each iteration, the edge weights considered by Dijkstra’s shortest path algorithm are t_a rather than t_f , reflecting congestion already on the road network.

For a given damage map, we compute the travel time between origins and destinations after assigning all trips demanded to the road network. For each origin-destination pair, we store the shortest-time path identified at each of the four iterations of the ITA algorithm. We then compute the travel time along each of those

four paths after the network has had 100% of trips assigned. To get the final travel time between the origin-destination pair, t_{OD} , we take the sum of the four paths’ travel times, each weighted by the percentage of the total trips assigned during that iteration, as shown in Equation (15).

$$t_{OD} = 0.4 \times t_{OD,1} + 0.3 \times t_{OD,2} + 0.2 \times t_{OD,3} + 0.1 \times t_{OD,4} \quad (15)$$

For a given damage map, the outputs of the traffic model include the travel time between each origin and destination and the number of trips made between each origin and destination. From these outputs, we can compute ΔT and the number of trips that were not made due either to infeasibility (because the origin and destination became disconnected as a result of bridge damage) or unacceptability (because the time required to make a trip exceeded t_{max}).

3.1.4 Welfare model

To estimate the welfare loss, ΔW , associated with a damage map, we specify the parameters of the welfare model in Equation (6). The income groups are determined by the structure of the LODES data set, which in the San Francisco Bay Area classifies 16% of commuters as having low incomes, 23% as having medium incomes, and 60% as having high incomes (U.S. Census Bureau, 2010). Although these classifications are associated with annual individual earnings ranges in LODES, those ranges are not San Francisco Bay Area-specific. Because Bay Area earnings are significantly different than nationwide averages, we estimate the bounds of each income group’s annual individual earnings range by averaging data on the San Francisco-Oakland-Fremont and San Jose-Sunnyvale-Santa Clara metropolitan areas from the U.S. Bureau of Labor Statistics. The resulting SVTT of Bay Area commuters is greater than that suggested by LODES earnings data by factors of 1.33, 1.35, and 1.1 for the low-, middle-, and high-income groups, respectively. We treat the SVTT of all members of an income group as a constant, in keeping with the resolution of the publicly available LODES data that we use, which includes only a commuter’s income group and not their actual annual individual earnings. For each income group, we use the midpoint of the associated earnings range to estimate SVTT and assume (per Belenky, 2011) that each commuter works 40 hours per week and 52 weeks per year to obtain their hourly wage, y , yielding the fifth column of Table 1. We use $\Omega = 1$ per Mackie et al. (2001). Layard et al. (2008) estimate the elasticity of the marginal utility of income $\rho = 1.26$. Per Equation (8), $\lambda = \frac{1}{y^\rho}$. Substituting our parameter values into Equation (6) yields Equation (16).

$$\Delta W = \sum_i \frac{1}{2y_i^{0.26}} \Delta T_i \quad (16)$$

If a trip is not made on a given damage map, the resulting welfare loss is calculated as the welfare loss that would result if the trip had taken t_{max} on the damage map.

3.1.5 Computational tractability

The primary determinants of the computational burden of this study are (1) the type of traffic model used; (2) the number of origins and destinations considered, which increases the complexity of the traffic assignment; and (3) the number of damage maps sampled, which determines the number of times traffic assignment must be performed. For each damage map, traffic assignment was performed on a node within a high-performance computing cluster (HPCC) with 16 CPUs and 64 GB of RAM per CPU and took 137 minutes on average. The change in welfare for members of each income group living in a census block and working in a census block was then computed for each damage map, taking 3 minutes on average on the same HPCC. If greater detail about individual network users is available, more sophisticated traffic models, such as activity-based travel demand models, may be worth their greater computational cost.

3.2 Regional welfare impacts of road network disruption

Because welfare losses are partly a function of increases in travel time, as Equation (6) specifies, we expect large ΔT will coincide with large ΔW in general, as Figure 3 shows. The principal advantage of setting up an analysis in which ΔW can be computed, however, is that the overall impact of road network disruption can be disaggregated into impacts on different groups of road network users, which can then be compared. For

Table 1: Comparison of SVTT for three income groups based on Bay-Area-specific Bureau of Labor Statistics individual earnings data.

Income group	Percentiles	Individual earnings [USD/year]	y [USD/h]	SVTT [USD/h]
Low	[0, 16)	0 - 23,251	4.8	2.4
Medium	[16, 39)	23,251 - 53,148	17.8	8.9
High	[39, 99]	53,148 - 552,455	52.8	26.4

example, Figure 3 also shows that for a given mean increase in travel time, commuters with low incomes will experience greater per-capita welfare losses than commuters with medium or high incomes. The disparity in Δw among the three groups of commuters is explained only in part by the difference in their SVTT values (shown in Table 1), as we will discuss further.

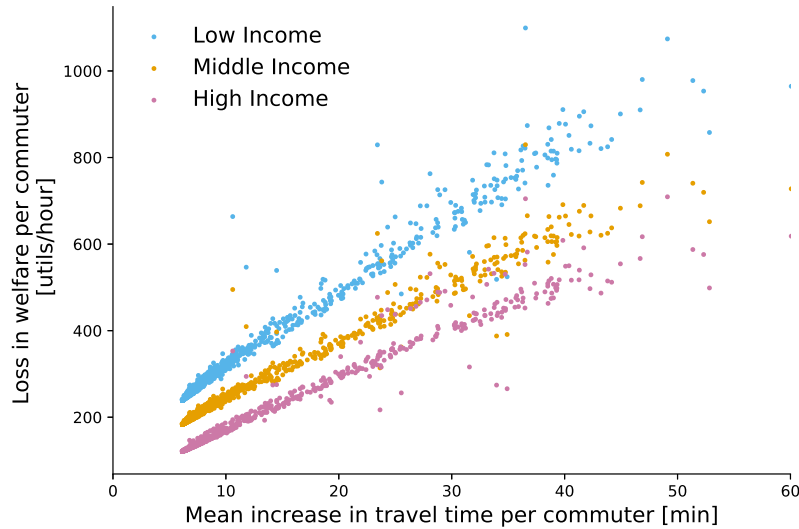


Figure 3: Comparison for each of $n_S = 1980$ earthquake scenarios of the mean increase in a commuter’s travel time [minutes], with the per-capita welfare loss for commuters in each income group, w_q [utils/hour].

Figure 4 shows the welfare loss exceedance curves for commuters in low-, medium-, and high-income groups assuming $t_{max} = 4$ hours. For each income group, the annual rate of exceedance of the welfare loss, $\lambda_{\Delta W}$, is computed using Equation (13). Figure 4a shows that members of the three income groups do not have significant differences in their risk of increased travel time per commuter. Figure 4b reveals that members of the low-income group have the greatest risk of welfare loss, while members of the high-income group have the least risk. While Figure 4 assumes $t_{max} = 4$ hours, our observation that commuters with low incomes are at greater risk of welfare loss than commuters with medium or high incomes also holds true when $t_{max} = 1, 2$, or 3 hours.

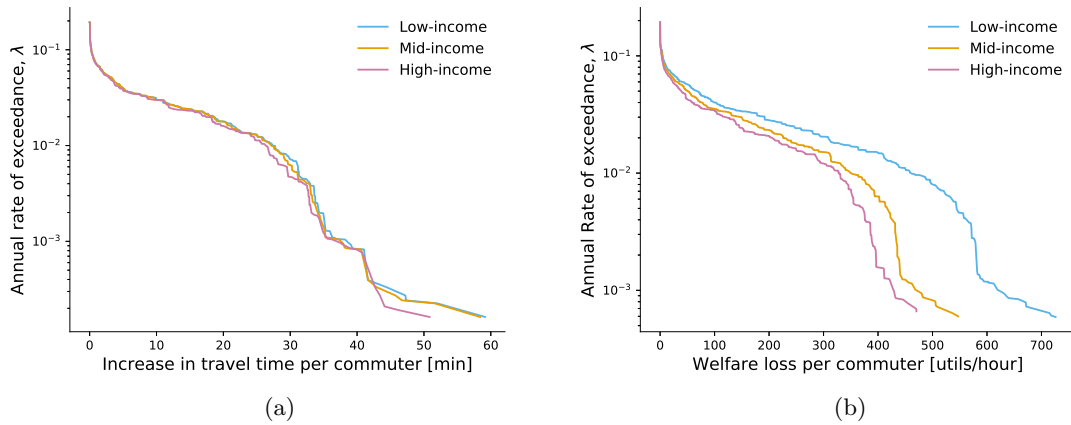


Figure 4: Comparison by income group of annual rate of exceedance curves for (a) increase in aggregate travel time per commuter on the road network and (b) per-commuter welfare loss. Both (a) and (b) assume a maximum acceptable one-way commute time of 4 hours.

Comparison of Figures 4a and 4b suggests that differences in the welfare loss exceedance curves of different income groups in Figure 4b stem in part from groups’ differing SVTT and λ_u . However, the ratio of the welfare loss per commuter (Δw_q) between income groups for each scenario is not equal to the ratio of the coefficient that multiplies ΔT in Equation (16). Figure 5 plots $\mathbb{E}[\Delta w_{low}]$ versus $\mathbb{E}[\Delta w_{high}]$ for each census block in the region of interest. The majority of the data points in Figure 5 differ significantly from the line that indicates the ratio of welfare coefficients that multiply ΔT_q in Equation (16). This indicates that the ratio between $\mathbb{E}[\Delta w_{low}]$ and $\mathbb{E}[\Delta w_{high}]$ is different than would be expected based on the ratio of the coefficients alone. Figure 5 also suggests that there is not a simple linear transformation between expected increase in travel time and expected welfare loss.

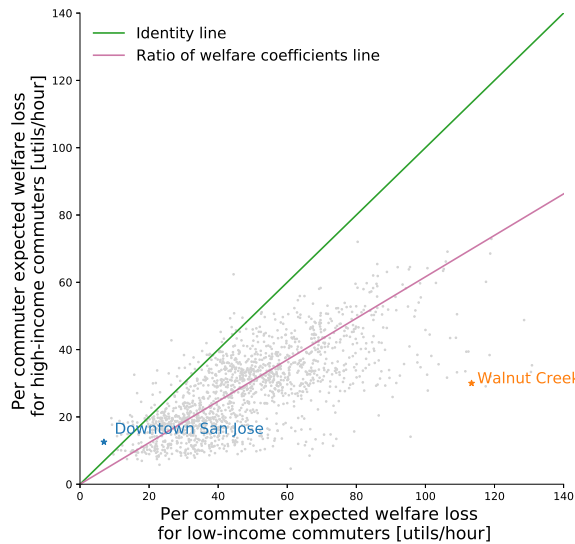


Figure 5: Scatter plot showing relation between low-income and high-income welfare per commuter loss per census blocks. Census blocks corresponding to San Jose and Walnut Creek are highlighted to show examples of areas of low and high disruption, respectively.

While loss exceedance curves aggregate information for the entire region of interest, Figures 6 and 7 map expected welfare loss per commuter living in and working in a census block, respectively. Expected welfare losses ($\mathbb{E}[\Delta W]$) were assessed on a census block level using Equation (10) (for Figure 6) and Equation (11) (for Figure 7) then normalized by the number of commuters living in or working in each census block to yield $\mathbb{E}[\Delta w]$, the expected welfare loss per commuter. Figure 6 shows that commuters living in the San Jose area experience the smallest expected welfare losses of all commuters in the region, while commuters living north of San Francisco and in the East Bay experience the highest $\mathbb{E}[\Delta w]$, across all income groups. Figure 2 suggests that the lower overall welfare losses in the San Jose area may result from greater network robustness there than in the North and East Bay regions.

Figure 7 shows that commuters working in the Peninsula and north of San Francisco experience the greatest $\mathbb{E}[\Delta w]$, while those working in the East Bay have lower $\mathbb{E}[\Delta w]$ across income groups. As in Figure 6, commuters with low incomes experience higher expected welfare losses than commuters in the mid- and high-income groups throughout the region of interest.

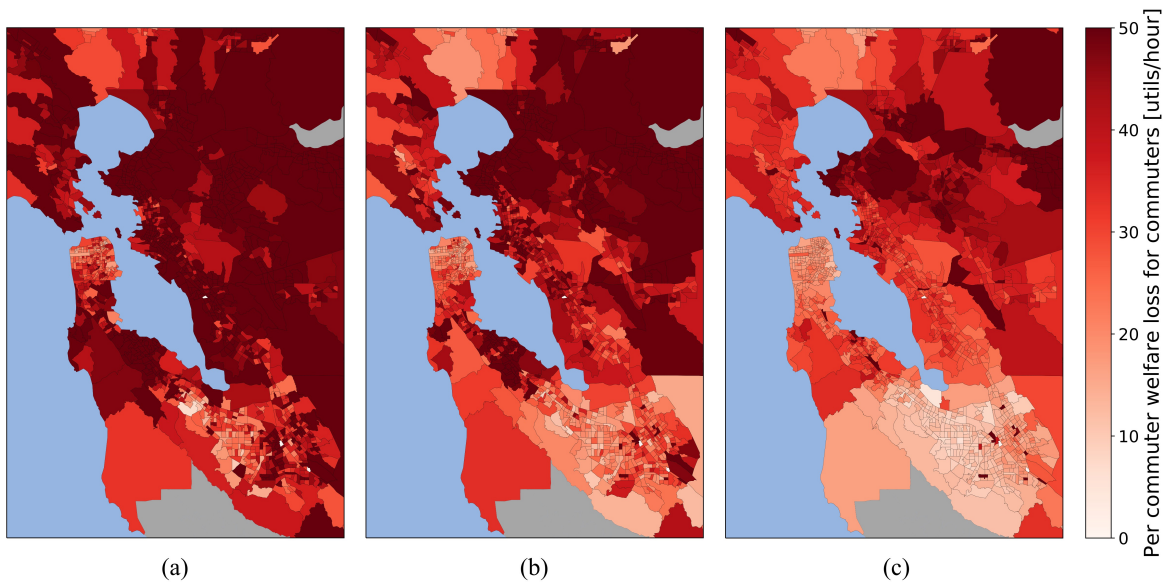


Figure 6: The expected welfare loss [utils/hour] per commuter living in a census block considering (a) only commuters with low incomes (b) only commuters with medium incomes (c) only commuters with high incomes.

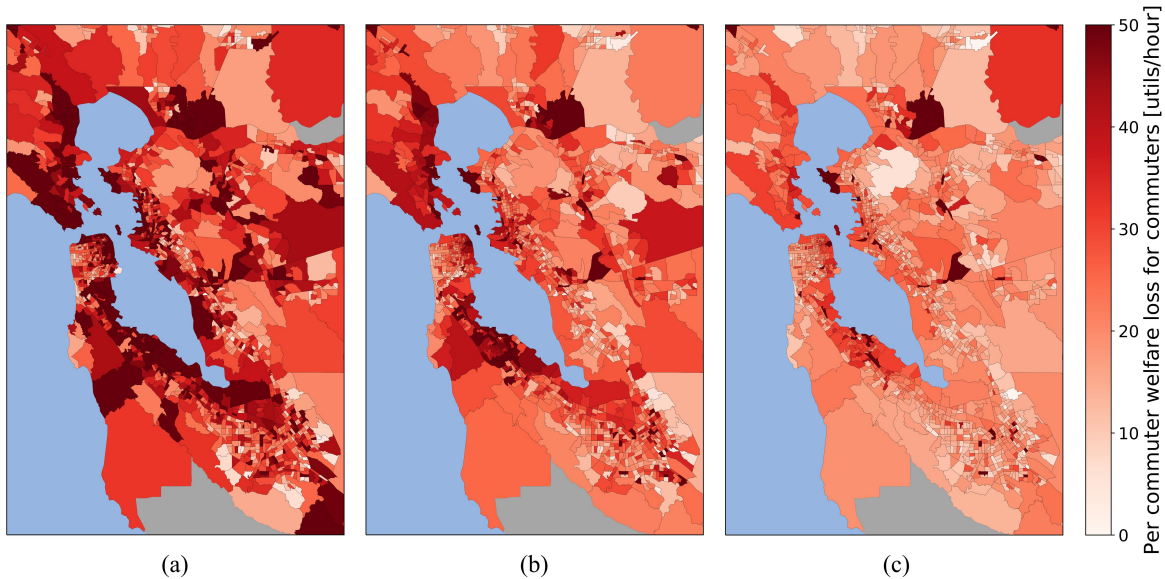


Figure 7: The expected welfare loss [utils/hour] per commuter driving to a census block considering (a) only commuters with low incomes (b) only commuters with medium incomes (c) only commuters with high incomes.

Figure 8 maps the difference between the expected welfare loss per commuter in a particular income group q living in a census block and the expected welfare loss per commuter considering all income groups in that census block, as summarized in Equation (17) (e.g., Keppel et al., 2005).

$$\frac{\mathbb{E}[\Delta w_q] - \mathbb{E}[\Delta w]}{\mathbb{E}[\Delta w]} \times 100\% \quad (17)$$

Census blocks shaded blue in Figure 8 are those in which the overall welfare loss per commuter ($\mathbb{E}[\Delta w]$) over-estimates the welfare loss per commuter of a particular income group, while census blocks shaded red are those in which $\mathbb{E}[\Delta w]$ under-estimates the welfare loss per commuter of a particular income group. Figures 8a and 8d show that $\mathbb{E}[\Delta w]$ consistently underestimates the expected welfare loss of commuters with low incomes, $\mathbb{E}[\Delta w_{\text{low}}]$. Conversely, Figures 8c and 8f show that $\mathbb{E}[\Delta w]$ overestimates the expected welfare loss of commuters with high incomes, $\mathbb{E}[\Delta w_{\text{high}}]$. This finding suggests that even when using measures of network performance that take into account how disruption may impact different network users to different degrees – such as welfare loss – aggregate statistics should be disaggregated by group-defining characteristics (e.g., income) so that between-group differences can be articulated and explored, as suggested by Bills and Walker (e.g., 2017). Figure 8 shows that, for this example, developing a network management policy using only $\mathbb{E}[\Delta w]$ would give more priority to the experience of commuters with high incomes than to the experience of commuters with low incomes.

Figure 8 also shows that the degree to which $\mathbb{E}[w]$ under- or overestimates the welfare loss of members of a particular income group varies spatially throughout the area of interest, in particular for commuters with low or medium incomes. Figure 8a indicates that $\mathbb{E}[\Delta w]$ underestimates $\mathbb{E}[\Delta w_{\text{low}}]$ more severely – i.e., by as much as 200% – for commuters living in the South Bay than for commuters living elsewhere in the Bay Area. Figure 8b indicates that $\mathbb{E}[\Delta w]$ underestimates $\mathbb{E}[\Delta w_{\text{mid}}]$ for commuters living in the South Bay but overestimates $\mathbb{E}[\Delta w_{\text{mid}}]$ for commuters living in most other locations. Disaggregation of welfare loss by the spatial unit of interest is therefore also important when assessing the impacts of road network disruption on groups of commuters.

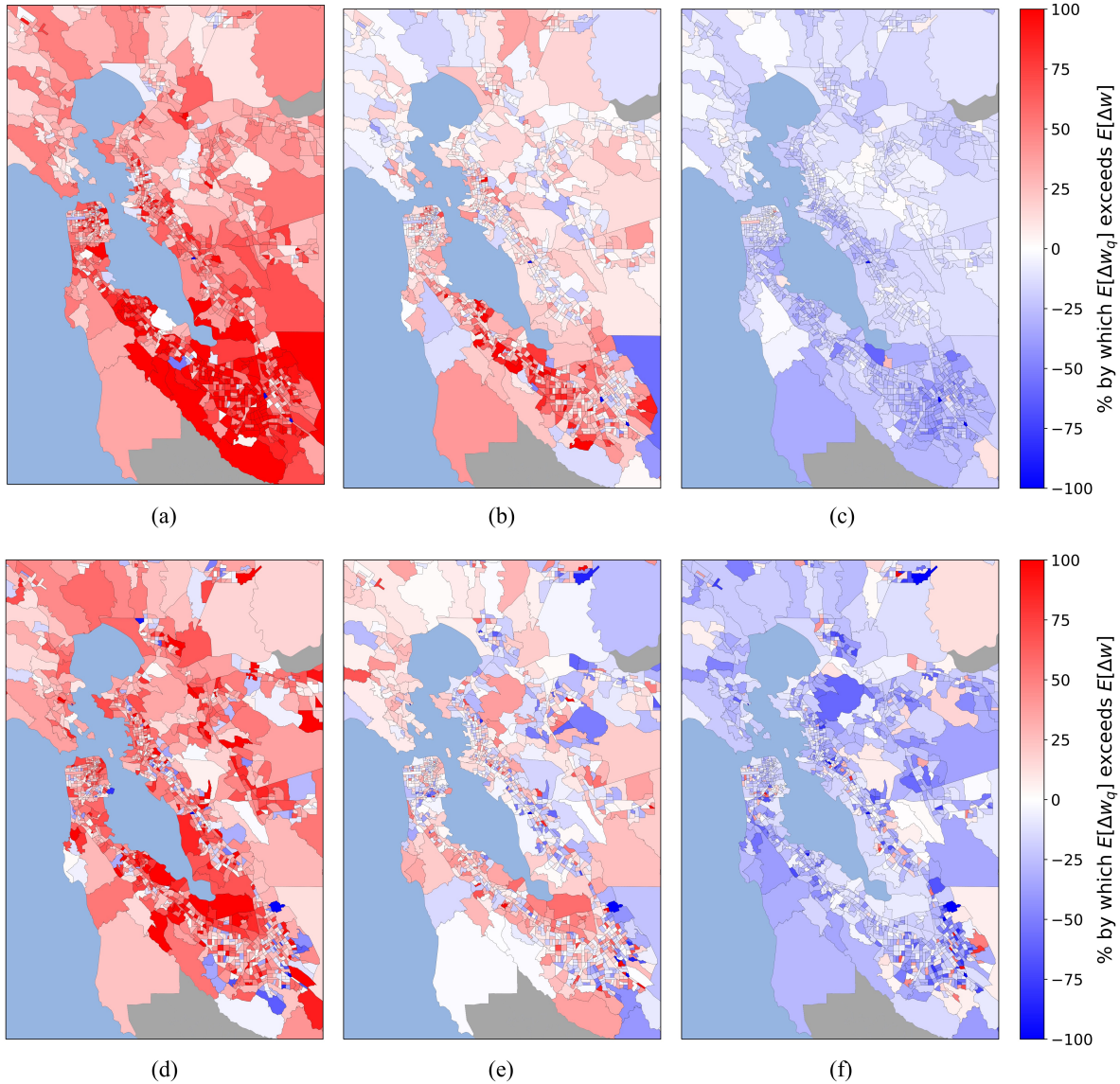


Figure 8: The percent by which the expected welfare loss per commuter among (a) commuters with low incomes ($\mathbb{E}[\Delta w_{low}]$) (b) commuters with medium incomes ($\mathbb{E}[\Delta w_{mid}]$) and (c) commuters with high incomes ($\mathbb{E}[\Delta w_{high}]$) exceeds the expected welfare loss per commuter when all commuters are considered together ($\mathbb{E}[\Delta w]$), as summarized in Equation (17). Figures (a), (b), and (c) show results for commuters living in particular census blocks, while Figures (d), (e), and (f) show results for commuters working in particular census blocks.

3.3 Effect of bridge retrofits

To illustrate how the use of welfare as a measure of road network performance may lead to more equitable decisions than using aggregate travel time, we compare the results of two simple bridge retrofit policies: a time-focused retrofitting (TFR) strategy and a welfare-focused retrofitting (WFR) strategy. The TFR strategy is determined by assessing the increase in aggregate travel time when each bridge in the road network is individually collapsed, a local sensitivity analysis method referred to as one-at-a-time analysis. Bridges are then prioritized for retrofit in decreasing order of their associated increase in aggregate travel time. To define the WFR strategy, we analyze the flow of commuters on the road network under normal conditions. We then rank bridges based on the proportion of commuters who use the bridge that have low incomes. The

higher the proportion of commuters with low-incomes who use a bridge, the higher the bridge is ranked.

Using each strategy, the 100 most important of the 1743 total bridges in the road network are retrofitted. The effect of retrofitting a bridge is modeled by multiplying the median value of its associated fragility function, f_b , by 1.2 (e.g., Padgett & DesRoches, 2009). This modeling choice is a simplification: as Padgett and DesRoches (2009) show, different seismic retrofit measures will have varying impacts on the fragility of a bridge. To evaluate the consequences of each retrofit strategy, the fragilities of the retrofitted bridges are updated and the probabilistic seismic risk assessment of the road network is repeated using the same 1980 scenarios. The effects of each retrofit prioritization strategy are assessed in terms of the welfare loss per capita (Δw) and the increase in aggregate travel time for the same hazard-consistent set of 1980 earthquake scenarios used earlier in this example, allowing us to obtain loss curves for each of these network performance measures.

Figure 9 shows that the WFR strategy decreases the impacts of road network disruption for commuters with low incomes more so than the TFR strategy. The WFR strategy does not decrease welfare losses for commuters with high incomes as much as the TFR. Based on this observation, we define the welfare loss ratio, ϕ_w , shown in Equation (18) as the ratio between the expected change in per-capita welfare for commuters with low incomes $E[\Delta w_{\text{low}}]$ and the expected change in per-capita welfare for commuters with high incomes $E[\Delta w_{\text{high}}]$. These expected values correspond to the areas under the associated loss exceedance curves in Figure 9.

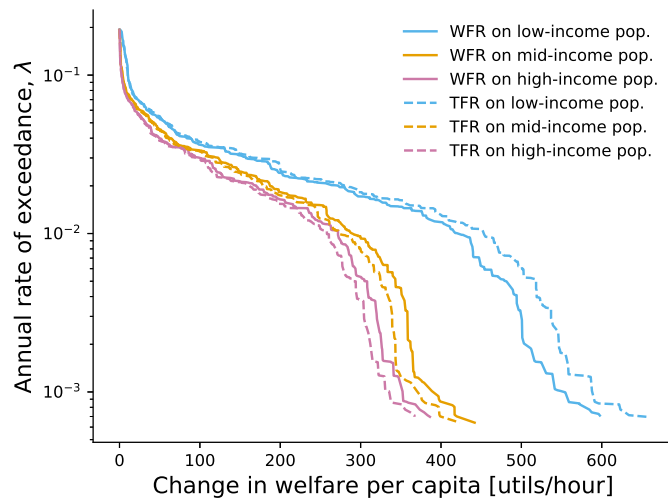


Figure 9: The effect of the time-focused retrofitting (TFR) strategy and the welfare-focused retrofitting (WFR) strategy on the per-capita welfare loss [utils/hour] of commuters in each income group.

$$\phi_w = \frac{\mathbb{E}[\Delta w_{\text{low}}]}{\mathbb{E}[\Delta w_{\text{high}}]} \quad (18)$$

While minimizing ϕ_w is not a desirable objective, examining its value for different strategies can be instructive. The use of ϕ_w allows us to compare the impacts of different policies on commuters in different income groups. Table 2 shows values of ϕ_w for different retrofitting strategies. For our testbed in the San Francisco Bay Area, using a TFR strategy increases the difference between the experiences of commuters with high incomes and commuters with low incomes compared to not retrofitting any bridges. In contrast, the WFR strategy decreases the difference between the two groups compared to a no-retrofit strategy. While the retrofit strategies and welfare loss ratio used in this example application are simple, they illustrate that different network management policies can have varying impacts on different groups of network users. More

sophisticated risk mitigation strategies could be designed on the basis of welfare losses among commuters in different income groups to ensure that all commuters share similarly in the benefits of those risk-reducing efforts. For example, minimizing Δw would be more desirable than minimizing ΔT .

Table 2: The effects of three bridge retrofit prioritization strategies on the welfare loss ratio in Equation (18).

Retrofit strategy	Welfare loss ratio, ϕ_w
No retrofits	1.6
Time-focused (TFR)	1.7
Welfare-focused (WFR)	1.5

4 Conclusions

In this study, we use welfare loss (as previously formulated by Mackie et al. (2001)) as a measure of post-earthquake road network disruption. Welfare is a metric that accounts for the impact of commute time on the well-being of commuters with varying incomes. We show how welfare loss can be integrated with a probabilistic seismic risk assessment framework in a computationally tractable way using publicly available data.

A probabilistic case study of commuters with low, medium, and high incomes in the San Francisco Bay Area shows that commuters with low incomes have disproportionately high expected welfare losses, while commuters with high incomes have disproportionately low expected welfare losses. Though welfare losses are correlated with drivers’ delay, the latter measure (and functions thereof) provides no insight into how commuters with different characteristics experience disruptions differently. Moreover, the case study shows that aggregate welfare losses underestimate the welfare losses of commuters with low incomes while overestimating the welfare losses of commuters with high incomes. This finding highlights the importance of using network performance metrics that (1) take into account differences in network users’ characteristics and (2) allow for disaggregation by those characteristics in order to understand the varying impacts of road network disruption on network users with different profiles.

Such disaggregation is also a prerequisite for equity analysis of network management policies. As shown in the case study, a bridge retrofit prioritization policy developed on the basis of drivers’ delay reduces the expected drivers’ delay but increases the disparity in the per-capita welfare loss of commuters with low and high incomes compared to the baseline network state, in which no bridges are retrofitted. In contrast, a bridge retrofit policy developed on the basis of the proportion of commuters that use a bridge and have low incomes reduces the disparity in the per-capita welfare loss of commuters with low and high incomes compared to the baseline network state.

Acknowledgements

We thank Maryia Markhvida and Adam Zsarnoczay for their feedback on earlier stages of this work. This work was supported in part by the Shah Fellowship on Catastrophic Risk at Stanford University. Some of the computing for this project was performed on the Sherlock cluster. We thank Stanford University and the Stanford Research Computing Center for providing computational resources and support that contributed to these research results.

Data availability

The code and data that support the findings of this study are openly available in a Github repository available in <https://zenodo.org/badge/latestdoi/433037407>

Declaration of interests

The authors have no conflicts of interest to disclose.

References

- Argyroudis, S., Selva, J., Gehl, P., & Pitilakis, K. (2015). Systemic seismic risk assessment of road networks considering interactions with the built environment. *Computer-Aided Civil and Infrastructure Engineering*, 30(7), 524–540. <https://doi.org/10.1111/mice.12136>
- Beckmann, M., McGuire, C. B., & Winsten, C. B. (1956). *Studies in the economics of transportation*. Yale University Press.
- Belenky, P. (2011). Revised Departmental Guidance on Valuation of Travel Time in Economic Analysis. *Office of Transportation Policy Reports*, 1–28.
- Bills, T. S., & Walker, J. L. (2017). Looking beyond the mean for equity analysis: Examining distributional impacts of transportation improvements. *Transport Policy*, 54(December 2016), 61–69. <https://doi.org/10.1016/j.tranpol.2016.08.003>
- Boakye, J., Guidotti, R., Gardoni, P., & Murphy, C. (2022). The role of transportation infrastructure on the impact of natural hazards on communities. *Reliability Engineering and System Safety*, 219. <https://doi.org/10.1016/j.ress.2021.108184>
- Bureau of Public Roads. (1964). *Traffic assignment manual for application with a large, high speed computer*. (tech. rep.). U.S. Department of Commerce, Urban Planning Division. Washington, D.C.
- Chang, L., Peng, F., Ouyang, Y., Elnashai, A. S., & Spencer, Jr., B. F. (2012). Bridge Seismic Retrofit Program Planning to Maximize Postearthquake Transportation Network Capacity. *Journal of Infrastructure Systems*, 18(2), 75–88. [https://doi.org/10.1061/\(ASCE\)IS.1943-555X.0000082](https://doi.org/10.1061/(ASCE)IS.1943-555X.0000082)
- Chang, S. E. (2016). Socioeconomic Impacts of Infrastructure Disruptions. *Oxford Research Encyclopedia of Natural Hazard Science*, (December), 1–27. <https://doi.org/10.1093/acrefore/9780199389407.013.66>
- Chiou, B. S.-J., & Youngs, R. R. (2014). Update of the chiou and youngs nga model for the average horizontal component of peak ground motion and response spectra. *Earthquake Spectra*, 30(3), 1117–1153.
- Decò, A., & Frangopol, D. M. (2013). Life-cycle risk assessment of spatially distributed aging bridges under seismic and traffic hazards. *Earthquake Spectra*, 29(1), 127–153. <https://doi.org/10.1193/1.4000094>
- Dong, Y., Frangopol, D. M., & Saydam, D. (2014). Pre-earthquake multi-objective probabilistic retrofit optimization of bridge networks based on sustainability. *Journal of Bridge Engineering*, 19(6), 1–10. [https://doi.org/10.1061/\(ASCE\)BE.1943-5592.0000586](https://doi.org/10.1061/(ASCE)BE.1943-5592.0000586)
- Faturechi, R., & Miller-Hooks, E. (2015). Measuring the Performance of Transportation Infrastructure Systems in Disasters: A Comprehensive Review. *Journal of Infrastructure Systems*, 21(1), 04014025. [https://doi.org/10.1061/\(asce\)is.1943-555x.0000212](https://doi.org/10.1061/(asce)is.1943-555x.0000212)
- Field, E. H., Dawson, T. E., Felzer, K. R., Frankel, A. D., Gupta, V., Jordan, T. H., Parsons, T., Petersen, M. D., Stein, R. S., Weldon, R., et al. (2009). Uniform California earthquake rupture forecast, version 2 (UCERF 2). *Bulletin of the Seismological Society of America*, 99(4), 2053–2107.
- Field, E. H., Jordan, T. H., & Cornell, C. A. (2003). OpenSHA: A developing community-modeling environment for seismic hazard analysis. *Seismological Research Letters*, 74(4), 406–419.
- Galvez, T., & Jara-Díaz, S. (1998). On the social valuation of travel time savings. *International Journal of Transport Economics*, 25(2), 205–219.
- Hackl, J., Adey, B. T., & Lethanh, N. (2018). Determination of Near-Optimal Restoration Programs for Transportation Networks Following Natural Hazard Events Using Simulated Annealing. *Computer-Aided Civil and Infrastructure Engineering*, 33(8), 618–637. <https://doi.org/10.1111/mice.12346>
- Hallegatte, S., Vogt-Schilb, A., Bangalore, M., & Rozenberg, J. (2016). *Unbreakable: Building the resilience of the poor in the face of natural disasters*. World Bank Publications.
- Han, Y., & Davidson, R. A. (2012). Probabilistic seismic hazard analysis for spatially distributed infrastructure. *Earthquake Engineering & Structural Dynamics*, 41, 2141–2158. <https://doi.org/10.1002/eqe>
- Jara-Díaz, S. R., & Guevara, C. A. (2003). Behind the subjective value of travel time savings: The perception of work, leisure, and travel from a joint mode choice activity model. *Journal of Transport Economics and Policy*, 37(1), 29–46.

- Silva-Lopez, R., Bhattacharjee, G., Poulos, A., and Baker, J. W. (2022). “Commuter welfare-based probabilistic seismic risk assessment of regional road networks.” *Reliability Engineering & System Safety*, 108730. <https://doi.org/10.1016/j.ress.2022.108730>
- Jayaram, N., & Baker, J. W. (2009). Correlation model for spatially distributed ground-motion intensities. *Earthquake Engineering & Structural Dynamics*, 38(15), 1687–1708.
- Keppel, K., Pamuk, E., Lynch, J., Carter-Pokras, O., Kim Insun, Mays, V., Percy, J., Schoenbach, V., & Weissman, J. S. (2005). Methodological issues in measuring health disparities. *Vital and health statistics. Series 2, Data evaluation and methods research*, (141), 1–16.
- Kilanitis, I., & Sextos, A. (2019a). Impact of earthquake-induced bridge damage and time evolving traffic demand on the road network resilience. *Journal of Traffic and Transportation Engineering (English Edition)*, 6(1), 35–48. <https://doi.org/10.1016/j.jtte.2018.07.002>
- Kilanitis, I., & Sextos, A. (2019b). Integrated seismic risk and resilience assessment of roadway networks in earthquake prone areas. *Bulletin of Earthquake Engineering*, 17, 181–210. <https://doi.org/10.1007/s10518-018-0457-y>
- Kiremidjian, A., Moore, J., Fan, Y. Y., Yazlali, O., Basoz, N., & Williams, M. (2007). Seismic risk assessment of transportation network systems. *Journal of Earthquake Engineering*, 11(3), 371–382. <https://doi.org/10.1080/13632460701285277>
- Layard, R., Nickell, S., & Mayraz, G. (2008). The marginal utility of income. *Journal of Public Economics*, 92(8-9), 1846–1857. <https://doi.org/10.1016/j.jpubeco.2008.01.007>
- Lindell, M. K., & Prater, C. S. (2003). Assessing Community Impacts of Natural Disasters. *Natural Hazards Review*, 4(4), 176–185. [https://doi.org/10.1061/\(ASCE\)1527-6988\(2003\)4](https://doi.org/10.1061/(ASCE)1527-6988(2003)4)
- Litman, T. (2002). Evaluating Transportation Equity. *World Transport Policy & Practice*, 8(2), 50–65.
- Mackie, P., Jara-Diaz, S., & Fowkes, A. (2001). The value of travel time savings in evaluation. *Transportation Research Part E*, (1965), 91–106.
- Miller, M. (2014). *Seismic Risk Assessment of Complex Transportation Networks* (Doctoral dissertation June). Stanford University.
- Miller, M., & Baker, J. W. (2016). Coupling mode-destination accessibility with seismic risk assessment to identify at-risk communities. *Reliability Engineering and System Safety*, 147, 60–71. <https://doi.org/10.1080/01944360208976274>
- Murphy, C., & Gardoni, P. (2006). The role of society in engineering risk analysis: A capabilities-based approach. *Risk Analysis*, 26, 1073–1083. <https://doi.org/10.1111/j.1539-6924.2006.00801.x>
- Padgett, J. E., & DesRoches, R. (2009). Retrofitted bridge fragility analysis for typical classes of multispan bridges. *Earthquake Spectra*, 25(1), 117–141. <https://doi.org/10.1193/1.3049405>
- Patriksson, M. (2015). *The Traffic Assignment Problem: Models and Methods*. Dover Publications, Inc.
- Petersen, M. D., Shumway, A. M., Powers, P. M., Mueller, C. S., Moschetti, M. P., Frankel, A. D., Rezaeian, S., McNamara, D. E., Luco, N., Boyd, O. S., Rukstales, K. S., Jaiswal, K. S., Thompson, E. M., Hoover, S. M., Clayton, B. S., Field, E. H., & Zeng, Y. (2020). The 2018 update of the us national seismic hazard model: Overview of model and implications. *Earthquake Spectra*, 36, 5–41. <https://doi.org/10.1177/8755293019878199>
- Small, K. A. (2012). Valuation of travel time. *Economics of Transportation*, 1(1-2), 2–14. <https://doi.org/10.1016/j.ecotra.2012.09.002>
- Small, K. A., & Verhoef, E. T. (2007). *The Economics of Urban Transportation*. Routledge.
- U.S. Census Bureau. (2010). LEHD Origin-Destination Employment Statistics Data.
- Wald, D. J., & Allen, T. I. (2007). Topographic slope as a proxy for seismic site conditions and amplification. *Bulletin of the Seismological Society of America*, 97(5), 1379–1395. <https://doi.org/10.1785/0120060267>
- Wang, P., Hunter, T., Bayen, A. M., Schechtner, K., & González, M. C. (2012). Understanding road usage patterns in urban areas. *Scientific Reports*, 2. <https://doi.org/10.1038/srep01001>
- Werner, S. D., Taylor, C. E., Cho, S., Lavoie, J.-P., Huyck, C. K., Eitzel, C., Chung, H., & Eguchi, R. T. (2006). *Redars 2 methodology and software for seismic risk analysis of highway systems* (tech. rep. MCEER-06-SP08). Multidisciplinary Center for Earthquake Engineering Research.
- Werner, S. D., Taylor, C. E., Moore, J. E., Walton, J. S., & Cho, S. (2000). *A Risk-Based Methodology for Assessing the Seismic Performance of Highway Systems* (tech. rep. MCEER-00-0014). Multidisciplinary Center for Earthquake Engineering Research.
- Zhou, Y., Banerjee, S., & Shinozuka, M. (2010). Socio-economic effect of seismic retrofit of bridges for highway transportation networks: A pilot study. *Structure and Infrastructure Engineering*, 6(1-2), 145–157. <https://doi.org/10.1080/15732470802663862>